

Composite spatial solitons in a saturable nonlinear bulk medium

C. Weilnau^{1,*}, W. Królikowski², E.A. Ostrovskaya³, M. Ahles¹, M. Geisser², G. McCarthy², C. Denz¹, Y.S. Kivshar³, B. Luther-Davies²

¹Institute of Applied Physics, Darmstadt University of Technology, Hochschulstr. 6, 64289 Darmstadt, Germany

²Laser Physics Centre, Australian National University, Canberra, ACT 0200, Australia

³Optical Sciences Centre, Australian National University, Canberra, ACT 0200, Australia

Received: 1 December 2000/Revised version: 12 January 2001/Published online: 21 March 2001 – © Springer-Verlag 2001

Abstract. We review the generation of the recently predicted multi-component spatial optical solitons in a saturable nonlinear bulk medium. We present numerical simulations for an effectively isotropic model and experimental results for a set of different combinations of a Gaussian beam co-propagating incoherently with a beam of a more complex internal structure, such as a higher order transverse laser mode. We discuss the different formation processes and the general properties of a variety of different dipole-mode composite solitons and expand our investigations to the generation of a quadrupole-mode composite soliton.

PACS: 42.65.Tg; 05.45.Yv; 42.65.Hw

Stable self-focusing of light in two transverse dimensions in a bulk nonlinear material has been a fast growing and attractive topic of research during the last decade [1]. The diffraction of a Gaussian beam is counterbalanced by a self-focusing effect in a material that exhibits a Kerr-like but saturable nonlinearity (e.g. a photorefractive nonlinear crystal). The beam shape remains constant during propagation, and it can be regarded as the fundamental Gaussian mode that propagates in its self-induced waveguide [2]. Self-trapped beams that consist of only one optical field are called scalar solitons, whereas vector or composite solitons represent the self-trapped beams that result from an incoherent superposition of several optical fields. Typically they consist of a fundamental Gaussian beam that co-propagates with one (or more) mutually incoherent higher-order mode of the induced multimode waveguide. Both beams remain mutually trapped due to the self-consistent change of the refractive index induced by both beams. Such types of spatial solitons have been extensively studied in the planar (1 + 1)D geometry [3]. Single and multi-hump structures as well as collision-induced shape transformation of the composite solitons have been demonstrated both experimentally and theoretically [4, 5]. Within the last year various configurations of composite solitons in two transverse

dimensions have been predicted theoretically [6, 7] and subsequently verified experimentally [8, 9]. Here, we give a review of the various classes of composite solitons that have been realized so far.

When expanding the problem to two transverse dimensions, the number of possible types of beams with different shapes becomes large. A Gaussian beam that induces a refractive index profile with an almost circular symmetry is expected to host higher-order-mode beams that are well-known from linear waveguide theory. Examples of these modes are depicted in Fig. 1. However, this linear principle can only be applied to multimode solitons if the higher-order mode is much weaker than the fundamental component that creates a multimode waveguide structure in which a less-intense probe beam is guided. Here we investigate composite structures that consist of two components of nearly equal intensity. The nontrivial question is whether these combined structures form a bound vector soliton state during propagation, or break apart forming several separated structures.

In this paper we analyze and observe experimentally three different kinds of two-dimensional spatial vector solitons. First, we review the generation of a dipole-mode vector soliton, which is a combination of a nodeless bell-shaped Gaussian fundamental component (Fig. 1a) with a Hermite–Gaussian (HG₁₀)-like dipole-mode (Fig. 1b). Second, we generate a similar dipole-mode vector soliton through the decay of a vortex beam of Laguerre–Gaussian (LG₀₁)-type (Fig. 1c) into a dipole-mode beam in the presence of a stabilizing Gaussian component. The resulting dipole-mode vector soliton displays a non-vanishing transverse angular momentum

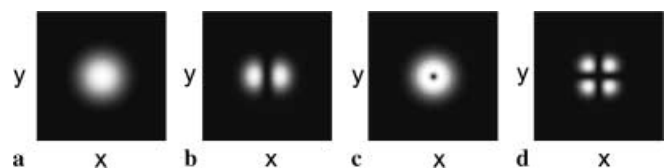


Fig. 1a–d. Examples of the transverse intensity distributions of the **a** fundamental, **b** dipole, **c** vortex and **d** quadrupole modes that become constituents of multi-component spatial optical solitons

*Corresponding author.

(Fax: +49-6151/164-123, E-mail: carsten.weilnau@physik.tu-darmstadt.de)

with its orientation depending on the sign of the topological charge of the initial vortex beam. Finally, we investigate the existence of quadrupole-mode vector solitons, where we combine the fundamental beam with a Hermite–Gaussian (HG₁₁) quadrupole-like mode (Fig. 1d) and discuss its stability and dynamics.

1 Theoretical approach

Our theoretical model is based on the isotropic approximation for screening solitons in a photorefractive material [10]. The interaction of two mutually incoherent beams in a bulk saturable nonlinear medium can be described by the normalized equations for the slowly varying beam envelopes:

$$i \frac{\partial E_{1,2}}{\partial z} + \Delta_{\perp} E_{1,2} - \frac{E_{1,2}}{1 + |E_1|^2 + |E_2|^2} = 0, \quad (1)$$

where Δ_{\perp} represents the transverse Laplacian and z is the propagation coordinate.

Here we restrict ourselves to the beam propagation method [11] to demonstrate the evolution of the multi-component solitary waves during propagation. As initial conditions for the Gaussian component we use $E_1(r) = A \exp[-r^2/(2a^2)]$ and for the dipole component $E_2(r) = Bx \exp[-r^2/(2b^2)]$ with A, B as the initial amplitude, a, b as the beam waist and $r = \sqrt{x^2 + y^2}$ as the radial transverse coordinate. Applying this to beam propagation, we obtain numerical solutions for the transverse intensity distribution after a certain propagation distance, z . In all cases we choose our parameters in order to get two initial beam profiles with equal total power.

First, let us combine a dipole-mode beam E_2 (Fig. 2a, top) with a mutually incoherent fundamental Gaussian beam E_1 (Fig. 2a, bottom). In the case when both components propagate separately in the nonlinear medium, the Gaussian beam remains self-focused and forms a solitary structure (Fig. 2b, bottom), whereas the two out-of-phase lobes of the dipole-mode beam strongly repel each other after the propagation of $z = 2$ (Fig. 2b, top). The situation changes drastically when both components co-propagate simultaneously in

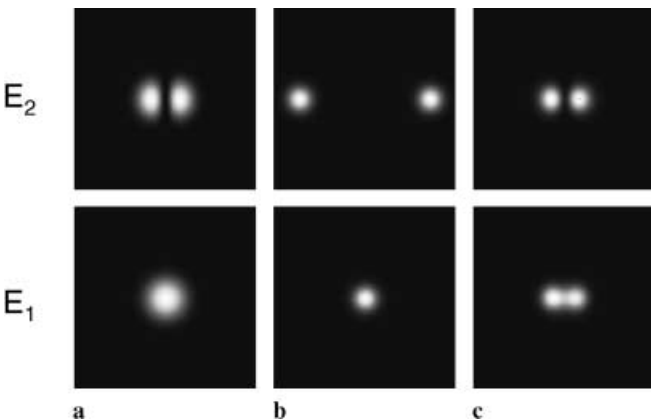


Fig. 2a–c. Numerical results: Creation of a dipole-mode vector soliton. *Top row:* the dipole (E_2) component, *bottom row:* the Gaussian (E_1) component. **a** Input intensity, **b** both components after independent propagation ($z = 2$) and **c** two stabilized components of the composite soliton when both beams co-propagate in the medium ($z = 6.95$)

the medium. The repulsion of the two dipole lobes is prevented (Fig. 2c, top) by the presence of the Gaussian component (Fig. 2c, bottom) and a stable dipole-mode vector soliton forms that survives for a large propagation distance of $z = 6.95$, which corresponds to almost 20 mm propagation distance in a real physical system. Propagation even further, up to several hundred diffraction lengths, shows that the trapped structure remains stable and does not break up.

Next, let us consider the propagation of an optical vortex (Fig. 1c), $E_2(r) = Br \exp[-r^2/(2b^2)] \exp(im\varphi)$, with a topological charge ($m = 1$). Its radial symmetric intensity distribution leads us to assume stable self-focusing when the vortex-bearing beam is propagating with a fundamental Gaussian component. But the linear stability analysis in [7] has proved that the radial symmetric solutions of (1) are linearly unstable. The vortex-component breaks up and decays into a dipole-mode with non-zero angular momentum. The instability growth rate is positive for any vanishingly small amplitude of this component, and it increases rapidly with the vortex intensity. Remarkably, an unstable vortex-mode soliton displays a symmetry-breaking instability. It always decays into a rotating radially asymmetric dipole-mode vector soliton which can survive for very long propagation distances. A simulated example of this behaviour is illustrated in Fig. 3. The top row reflects the vortex component (E_2) and the corresponding fundamental component (E_1) is shown in the bottom row. Figure 3a (top and bottom) shows the input intensity distribution. In Fig. 3b one can see both components after separate propagation for $z = 5.9$. The initial circular symmetric transverse shape of the vortex displays a modulational instability-induced decay into four single peaks. Figure 3c demonstrates the behaviour when both components co-propagate and interact incoherently ($z = 12$). In the presence of the Gaussian beam, the vortex does not break apart into several peaks but remains in a metastable state for a certain propagation distance ($z < 9$). When it propagates further ($z = 12$), it decays into a stable counter-clockwise rotating dipole structure, and its Gaussian E_1 component becomes elliptically shaped (Fig. 3c). Figure 3d and e show the intensity distribution for the propagation lengths $z = 12.3$ and $z = 12.6$ and demonstrate the rotational nature of the dipole-mode vector soliton. A more continuous rotation over several hundred diffraction lengths is illustrated in [7].

When changing the sign of the topological charge of the vortex to $m = -1$, we change the orientation of its screw-like

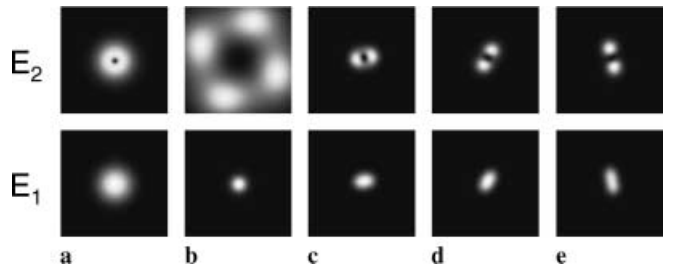


Fig. 3a–e. Numerical results: Creation of a dipole-mode vector soliton after the decay of an unstable vortex beam ($m = 1$). *Top row:* the vortex component, *bottom row:* the Gaussian component. **a** Input intensity, **b** both components after independent propagation ($z = 5.9$). Simultaneous propagation leads to the formation of a stable and rotating dipole-mode vector soliton for **c** $z = 12$, **d** $z = 12.3$ and **e** $z = 12.6$

transverse phase distribution. Therefore the angular momentum of the dipole-mode vector soliton which is induced by the vortex will change its direction as well. Figure 4 depicts the result of a simulation where $m = 1$ was replaced by $m = -1$. Figure 4a–c correspond to Fig. 3d–e and display now a clockwise rotation of the dipole structure, as expected.

The robustness of the dipole-mode structure encourages us to seek higher-order modes that can remain trapped by a co-propagating Gaussian beam. Below, we investigate the evolution of a pair of coupled dipoles forming a quadrupole mode as is depicted in Fig. 1d. In contrast to the dipole-mode beam (Fig. 1b), the quadrupole-mode that resembles a Hermite–Gaussian (HG_{11}) mode (Fig. 1d) has a π phase jump across both transversal directions x and y . Again we perform a numerical beam propagation using the ansatz $E_2(r) = Bxy \exp[-r^2/(2b^2)]$.

The result is illustrated in Fig. 5. In the absence of the Gaussian beam, the single lobes of the quadrupole form four self-focused light spots that repel each other after a certain propagation distance ($z = 4.7$), which is equivalent to the case of the dipole-mode beam in Fig. 2. Again, the Gaussian beam stabilizes the whole structure, the four intensity humps of the quadrupole-mode component remain trapped and a stable quadrupole-mode vector soliton forms.

Given the results of our theoretical analysis, it is natural to ask whether the effects observed in the numerical simulations represent fundamental phenomena that can be observed experimentally.

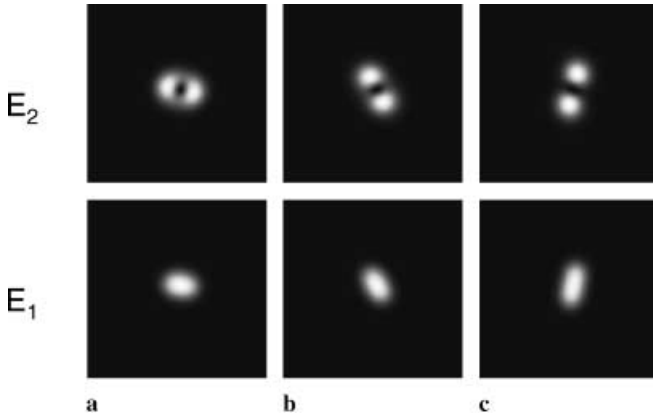


Fig. 4a–c. Numerical results: Creation of a dipole-mode vector soliton from the decay of a negatively charged vortex ($m = -1$). The general behaviour is the same as in Fig. 3 but the orientation of the rotation has changed. Simultaneous propagation of both beams is shown for **a** $z = 12$, **b** $z = 12.3$, and **c** $z = 12.6$

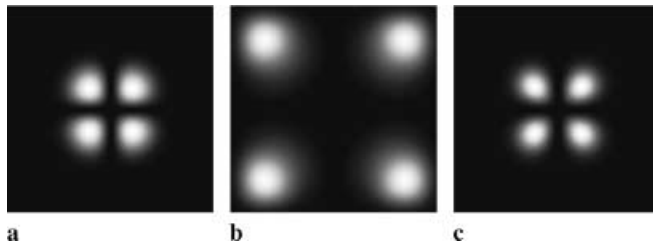


Fig. 5a–c. Numerical results: Creation of a quadrupole-mode composite soliton. Here, only the quadrupole component is shown. **a** Input intensity, **b** separate propagation of the quadrupole mode and **c** propagation of the quadrupole mode in the presence of the fundamental component ($z = 4.7$)

2 Experimental approach

The experimental setup to generate different multipole vector solitons is a standard one [8], and for consistency it is shown in Fig. 6. We derive two beams from a Nd:YAG laser ($\lambda = 532$ nm). With the help of a Mach–Zehnder-like arrangement consisting of two beamsplitters (BS1, BS2) and two mirrors (M1, M2). One of the beams is transmitted through a computer-generated phase mask or a series of thin glass slides in order to obtain the required transversal phase distribution for the vortex, dipole or quadrupole beam. In this way, we can generate a vortex beam with a doughnut-like shape, a vanishing intensity in its center and a screw-like phase distribution with a topological charge of $m = \pm 1$. To generate a dipole beam, we partially insert a glass slide in the beam to induce a π phase shift across its transverse plane in such a way that the dipole is oriented perpendicular to the c -axis of the crystal. For the quadrupole beam, we use an additional glass slide that is inserted in a direction perpendicular to that of the first one.

The second beam, bearing the Gaussian fundamental mode, is reflected by a mirror mounted on a piezoelectric transducer which is driven by an AC voltage at a frequency of approximately 1 kHz. The crystal has a non-instantaneous temporal response to varying light intensity, and therefore a high response time τ , in the range of seconds. It cannot follow the intensity fluctuations of the interference pattern that result from the oscillating mirror. Due to this technique both beams become effectively incoherent to each other. They are both linearly polarized in the direction of the crystal's c -axis, combined with a second beamsplitter (BS2), and focused onto the input face of the crystal.

We use three different samples of photorefractive SBN crystals doped with cerium (0.002% by weight). Their dimensions ($a \times b \times c$) are ($10 \times 6 \times 5$) mm, ($15 \times 8 \times 5$) mm and ($13.5 \times 5 \times 5$) mm. They are biased with a DC electric field of 0.7–2 kV along their c -axis, which is perpendicular to the propagation direction in order to obtain a focusing nonlinearity of saturable type. To control the degree of saturation, we illuminate the crystal homogeneously with incoherent white light. It can be estimated that the degree of saturation is in the range of unity for all our experiments. Finally, the exit face of the crystal is imaged with a lens (L2) on a CCD camera and the data are processed using a computer system.

Figure 7 shows the generation of a dipole-mode composite soliton. The single figures are in the same order as the ones illustrating the numerical simulations (Fig. 2). When launching a dipole-mode beam into the DC-electric-field-biased SBN crystal, the two out-of-phase lobes form a local-

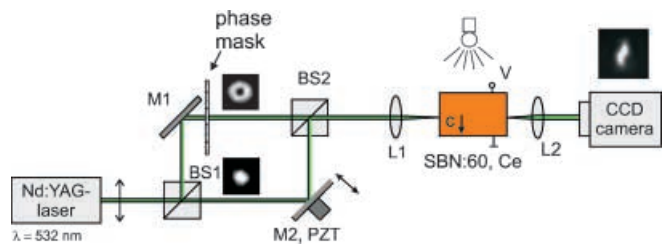


Fig. 6. Sketch of the experimental setup, illustrating the Mach–Zehnder arrangement consisting of beamsplitters BS1 and BS2 and mirrors M1 and M2

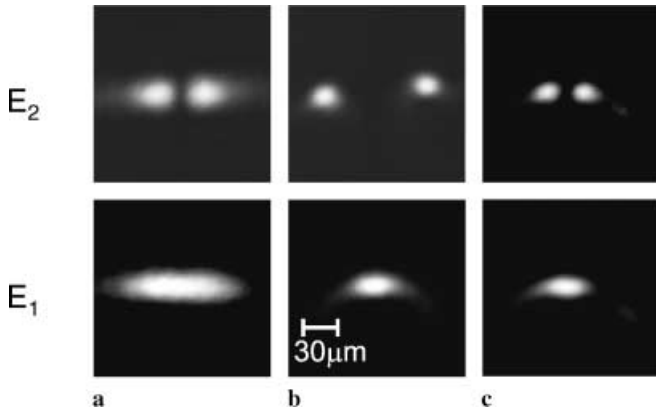


Fig. 7a–c. Experiment: Generation of a dipole-mode composite soliton (c) from two out-of-phase lobes that strongly repel each other (b). Parameters are $z = 15$ mm, $V = 2$ kV, and initial powers $P_{E_1} = P_{E_2} = 0.6$ μ W

ized structure and repel each other strongly (Fig. 7b, top). The presence of the Gaussian beam prevents this repulsion and allows both beams to become constituents of the dipole-mode soliton. The Gaussian component passes a system of cylindrical lenses in order to form an elliptically shaped Gaussian beam (Fig. 7a, bottom) which is able to cover the whole intensity distribution of the dipole mode generated by passing partially through a thin glass slide. The external electric field of $V = 2$ kV is oriented in the vertical direction.

To observe both co-propagating components separately (see Fig. 7c), we make use of the slow response time of the photorefractive crystal. When both components are present in the material, and the stable vector soliton has formed, we block one of the beams and immediately record ($\Delta t \approx 0.1$ s) the remaining light intensity from the other beam. Within this short time interval, the induced index structure cannot change significantly, which allows us to detect one of the two components separately.

As already demonstrated in Fig. 3 and [7], the second method to obtain a dipole-mode composite soliton is via the decay of an unstable vortex beam in a bulk nonlinear medium [12]. For this purpose, we modify our setup and replace the glass slide by a computer-generated phase mask that produces a vortex with charge $m = \pm 1$ in the ± 1 st diffraction order. Additionally, we change the crystal's orientation. The beam propagates along the 5 mm long b -axis and the electric field which is parallel to the crystal's c -axis points in the horizontal direction.

When we launch the vortex ($m = 1$) into the biased crystal (Fig. 8a, top), the beam does not self-trap but displays an instability. As a consequence, it forms some irregularly and not very clearly focused spots (Fig. 8b, top). But when the Gaussian beam is co-propagating in a mutually incoherent way with the vortex, the break-up is prevented, and a distinct focused two-peak structure forms that aligns at an angle of 42° with respect to the vertical axis (Fig. 8c, top). When we perform the same experiment but use the -1 st diffraction order of our phase mask, we produce a vortex with $m = -1$. The break-up of this beam for a separate propagation is nearly the same as in the case of the positively charged one (Fig. 8b). But the combined propagation with the Gaussian beam produces a dipole-mode vector soliton that rotates in the opposite direction (Fig. 8d) and aligns at an angle of -39° with respect

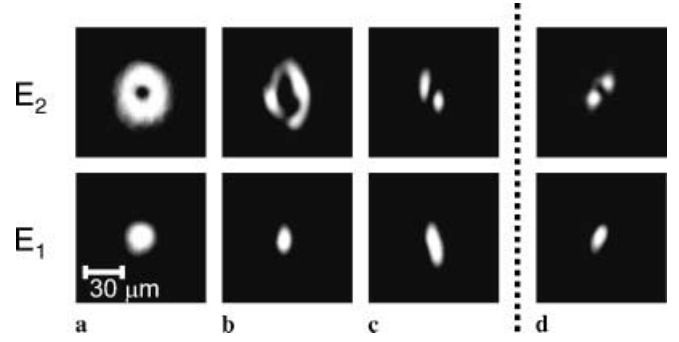


Fig. 8a–d. Experiment: Generation of a dipole-mode composite soliton via the decay of an unstable vortex beam (b, top), for the case of a vortex with $m = 1$ (c, top) and $m = -1$ (d, top). Parameters are $z = 5$ mm, $V = 1.6$ kV, and initial powers $P_{E_1} = 2.2$ μ W and $P_{E_2} = 1.8$ μ W

to the vertical axis. It is interesting to mention here that also the shape of the fundamental Gaussian component is affected and becomes slightly elliptically elongated in the direction of the dipole axis (Fig. 8c,d, bottom). This is an indication that the principle of self-consistency is really valid in this case. The dipole does not populate a mode that is induced by a multimode waveguide resuming from the Gaussian beam, but both beams induce a self-consistent refractive index structure that supports their stable self-focusing.

In Fig. 9, we prove that the observed two-peak structures in both experiments are of a dipole type. For this purpose the dipole-bearing part (Fig. 9a,c) of the vector soliton is superimposed with a coherent plane wave. Figure 9b and d show that the interference fringes for both lobes are shifted about π , proving the dipole nature of this components of the vector soliton.

Finally, we investigate the generation of a quadrupole-mode vector soliton. Similar to the experiments with the direct imprinting of the dipole onto one of the beams (see Fig. 7a, top), we insert an additional glass slide perpendicular to the first one into the dipole beam. Using this method we obtain a transverse profile consisting of four humps with a relative phase difference of π (Fig. 10a, top). After launching this beam into the biased crystal, four clearly separated light intensity peaks form after a propagation distance of 13.5 mm (Fig. 10b, top). When the fundamental Gaus-

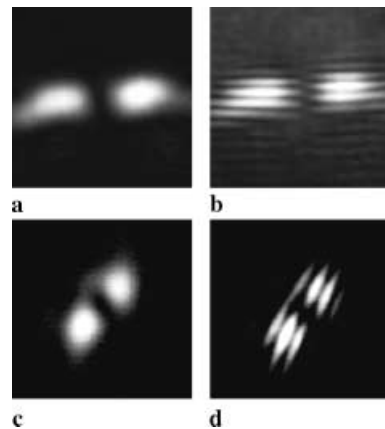


Fig. 9a–d. Experiment: Interference patterns (b,d) of the two dipole-components (a,c) with a mutually coherent plane wave. The shift in the fringes indicates that both structures are π out of phase

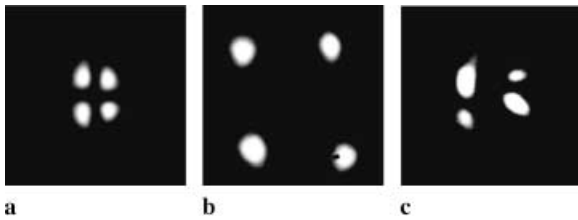


Fig. 10a–c. Experiment: Generation of a quadrupole-mode composite soliton (c) derived from four out-of-phase humps (a) that become separated after propagating in the crystal (b). The Gaussian component is not shown here. Parameters are $z = 13.5$ mm, $V = 0.7$ kV, and initial powers $P_{E_1} = 0.9$ μ W and $P_{E_2} = 1.1$ μ W

sian beam is launched simultaneously, the four peaks remain trapped during propagation (Fig. 10c). In contrast to the case of the dipole-mode soliton, it is important to mention that the quadrupole mode could not be obtained as distinctly as for the case of the dipole mode. We believe that the reason for this lies in the imperfectness of our sample, in the inherent anisotropy of the photorefractive crystal and in a slight misalignment of the two beams. Even the simulations in an isotropic medium reveal that a slight misalignment of the two beams leads to a complex propagation behaviour. In the experiment, the shape as well as the alignment of the beams can only be realized up to a certain accuracy. Further investigations to improve these results are in progress.

3 Discussion and conclusion

The experimental results shown above (see Figures 7–10) are in a good qualitative agreement with the numerical simulations depicted in Figures 2–5. The predicted dipole-mode vector soliton can be realized experimentally. Both methods, the direct phase imprinting (see Fig. 7) and the vortex decay (see Fig. 8), lead to the generation of a stable dipole-mode vector soliton. It is surprising that a radially symmetric structure (the vortex-mode soliton) decays into a radially asymmetric structure (the dipole-mode soliton) which is more stable in a saturable bulk nonlinear medium. The nonvanishing angular momentum of the dipole-mode vector soliton that originates from the decay of the vortex could be demonstrated numerically by illustrating different stages of its propagation (Figs. 3 and 4). It is very difficult to observe such a spiraling motion of the beamlets in the experiment due to the inherent anisotropy of our photorefractive nonlinear crystal [13]. The symmetry of the system is strongly perturbed, and we

observe that the dipole peaks only align at one characteristic angle, indicating a clockwise rotation for a topological charge of $m = -1$ and a counter-clockwise rotation for $m = 1$, which corresponds to the results of the simulations depicted in Figs. 3 and 4. We believe that the anisotropic nonlinearity also supports the break up of the circular symmetric structure of the vortex into several beamlets for a quite short propagation distance ($z = 5$ mm), whereas the simulations of the isotropic model display a break up for $z > 9$, which corresponds to more than 20 mm.

In conclusion we have reviewed the existence of a new kind of optical spatial solitons in a saturable bulk nonlinear medium. These dipole-mode vector solitons are circularly asymmetric but much more stable than the corresponding radially symmetric vortex-mode vector soliton. Moreover, we demonstrated the possibility to generate vector solitons consisting of a fundamental and a higher-order mode, as demonstrated with a quadrupole-mode beam.

Acknowledgements. The authors acknowledge support from the Performance and Planning Fund of the Australian National University, the Australian Photonics CRC, the German Academic Exchange Service (DAAD) and the FAZIT foundation.

References

1. For an overview, see G.I. Stegeman, M. Segev: *Science* **286**, 1518 (1999)
2. A.W. Snyder, D.J. Mitchell, L. Poladian, F. Landoucheur: *Opt. Lett.* **16**, 21 (1991)
3. See, for example, M. Mitchell, M. Segev, D.N. Christodoulides: *Phys. Rev. Lett.* **80**, 4657 (1998)
4. M. Mitchell, M. Segev, T.H. Coskun, D.N. Christodoulides: *Phys. Rev. Lett.* **79**, 4990 (1997)
5. W. Królikowski, N.N. Akhmediev, B. Luther-Davies: *Phys. Rev. E* **59**, 4654 (1999)
6. Z.H. Musslimani, M. Segev, D.N. Christodoulides: *Phys. Rev. Lett.* **84**, 1164 (2000); Z.H. Musslimani, M. Segev, D.N. Christodoulides: *Opt. Lett.* **25**, 61 (2000)
7. J.J. García-Ripoll, V. Pérez-García, E.A. Ostrovskaya, Yu.S. Kivshar: *Phys. Rev. Lett.* **85**, 82 (2000)
8. W. Królikowski, E.A. Ostrovskaya, C. Weir, M. Geisser, G. McCarthy, Yu.S. Kivshar, C. Denz, B. Luther-Davies: *Phys. Rev. Lett.* **85**, 1424 (2000)
9. T. Carmon, C. Anastassiou, S. Lan, D. Kip, Z.H. Musslimani, M. Segev: *Opt. Lett.* **25**, 1113 (2000)
10. D.N. Christodoulides, S.R. Singh, M.I. Carvalho, M. Segev: *Appl. Phys. Lett.* **68**, 1763 (1996)
11. T. Taha, M.J. Ablowitz: *J. Comp. Phys.* **55**, 203 (1994)
12. V. Tikhonenko, J. Christou, B. Luther-Davies: *Phys. Rev. Lett.* **76**, 2698 (1996)
13. A.A. Zozulya, D.Z. Anderson: *Phys. Rev. A* **51**, 1520 (1995)